Boundary-Layer Meteorol
DOI 10.1007/s10546-008-9320-z

NOTE

On the Possible Impact of a Following-Swell on the Atmospheric Boundary Layer

V. K. Makin

Received: 3 March 2008 / Accepted: 11 September 2008

Abstract A simple model of the atmospheric boundary layer over the ocean where the swell impact on the atmosphere is explicitly accounted for is suggested. The model is based on Ekman's equations, where the stress in the wave boundary layer is split into two parts: the turbulent and wave-induced stress. The turbulent stress is parameterized traditionally via the eddy viscosity proportional to the generalized mixing length. The wave-induced stress directed upward (from swell to the atmosphere) is parameterized using the formalism of the wind-over-waves coupling theory. The model can be seen as an extension of the model by Kudryavtsev and Makin (J Phys Oceanogr **34**:934–949, 2004) to the scale of the entire atmospheric boundary layer by including the Coriolis force into the momentum conservation equation and generalizing the definition of the mixing length. The regime of low winds for swell propagating along the wind direction is studied. It is shown that the impact of swell on the atmosphere is governed mainly by the swell parameter—the coupling parameter that is the product of the swell steepness and the growth rate coefficient. When the coupling parameter drops below -1 the impact of swell becomes significant and affects the entire atmospheric boundary layer. The turbulent stress is enhanced near the surface as compared to the no-swell case, and becomes negative above the height of the inner region. The wind profile is characterized by a positive gradient near the surface and a negative gradient above the height of the inner region forming a characteristic bump at the height of the inner region. Results of the model agree at least qualitatively with observations performed in the atmosphere in presence of swell.

Keywords Atmospheric boundary layer · Low wind speeds · Swell · Wave boundary layer

1 Introduction

Swell is a common feature on the ocean surface. It originates from dying storms when long waves in the peak of the wave spectrum cease receiving energy from the rapidly falling

V. K. Makin (✉)
Royal Netherlands Meteorological Institute, De Bilt, The Netherlands
e-mail: makin@knmi.nl

wind and radiate from the origin of the storm. It can propagate thousands of km crossing whole oceans (Munk et al. 1963; Snodgrass et al. 1966), but attenuates due to its interaction with the local wind fields, bottom and boundary friction, and other mechanisms. Crossing tropical oceans, swell normally propagates in the environment of low wind speeds. It was commonly thought that swell does not interact with the air flow and has no impact on the marine atmospheric boundary layer (ABL). In the last decade this point of view has changed as new experimental evidence becomes available. It appears that swell does interact with the atmosphere losing energy and momentum to the wind.

Yelland and Taylor (1996) found that in the open ocean at low wind speeds, the drag coefficient increases with a decrease in the wind speed below $5\,\mathrm{m\,s^{-1}}$. This rather rapid increase cannot be explained by the aerodynamically smooth conditions of the sea surface. The authors mentioned that the cruise area was characterized by large swell waves, and during the cruise swell was a dominant feature of the ocean surface at low to moderate wind speeds. So, swell could be responsible for this increase. Unfortunately, the direction of the swell propagation and other swell parameters were not measured or reported from visual observations. Besides, this dataset is known to be affected by the flow distortion over the ship (Yelland et al. 1998). It is also not clear that stress estimates via the inertial dissipation method are able to discern swell effects.

Donelan et al. (1997) found a strong increase in the drag coefficient at low wind speeds in the presence of swell propagating opposite to the wind. The number of following-swell (direction of swell coincides with the direction of the wind) cases was too low to warrant any conclusions, though the results were confirmed by Drennan et al. (1999a, b).

Guo-Larsen et al. (2003) observed the reduction of the drag coefficient in the case of a following-swell and low wind speeds in the Baltic Sea. The same feature was observed during the CBLAST experiment as reported by Sullivan et al. (2008).

Another phenomenon, which points to the impact of swell on the atmosphere, is the upward momentum transfer, directed from swell to the wind, that occurs when swell propagates faster than the wind and its direction coincides with the wind direction. The upward momentum transfer leads to wave-driven winds—acceleration of the airflow close to the sea surface—as compared to no-swell conditions.

In laboratory conditions a wave-driven wind was observed by Harris (1966), who showed that progressive waves propagating in still air induce a mean wind in the direction of wave propagation. A comprehensive study of the upward momentum flux at low wind speeds and in the presence of swell over the open ocean is reported by Grachev and Fairall (2001). For a following-swell and a wind speed below $2\,\mathrm{m\,s^{-1}}$ they observed a clear signature of the upward total momentum flux at measurement heights exceeding 10 m, implying that the wind profile has a maximum at a height below 10 m. Grachev and Fairall (2001) provided also an extensive overview of relevant studies. Here, it is mentioned only that Smedman et al. (1994) reported a momentum flux directed upwards in the lowest 200 m of the ABL, which corresponds to a negative wind gradient (their Figs. 3 and 4). The measurements were made at heights exceeding 30 m. A negative gradient of the wind speed evaluated at 10-m height from a best fit of the wind speed measured at five heights between 10 m and 28 m is reported by Smedman et al. (1999). This implies that the wind profile has a maximum at a height below 10 m.

The fact that the upward momentum flux does exist was known rather long ago. Numerical studies of wind-wave interaction (e.g., Gent and Taylor 1976; Makin 1980) showed that waves propagating faster than the wind are characterized by a negative wave growth rate, i.e. losing energy and momentum to the wind. The existence of the wave-driven wind is easily explained following the reasoning of Makin and Mastenbroek (1996). Let us integrate the equation for the mean horizontal momentum in the constant-flux surface layer

$$\frac{\partial}{\partial t}\int_{\eta}^{\delta_W} u dz = \tau_{\delta_W} - \tau_s, \tag{1}$$

where u is the mean horizontal velocity component, z is a vertical coordinate, η is the surface elevation, subscript s denotes the surface fluxes, $z = \delta_W$ is defined as the height where the wave-induced stress is negligible (wave boundary layer or WBL), so that the stress at that height is supported only by the turbulent stress $\tau_{\delta_W} = \tau^t = u_*^2$, and by definition equals the square of the friction velocity u_*. At the surface the total stress has two components: the turbulent and wave-induced $\tau_s = \tau_s^t + \tau_s^w$. Assuming a stationary situation without the wave-induced stress initially, the introduction of the negative wave-induced stress τ_s^w due to swell at the surface implies that the flow inside δ_W will accelerate unless the balance (1) is satisfied. Since, at the surface, the mean velocity is zero and kept constant at $z = \delta_W$, the velocity profile can no longer be logarithmic but is characterized by a positive bump. The deviation of this profile from the logarithmic law is called the wave-driven wind.

Kudryavtsev and Makin (2004) suggested a model of swell interaction with the airflow based on the two-layer approximation of the wave boundary layer (WBL). They were able to explain the increase of the drag coefficient in opposite-swell cases and the formation of the jet-like wave-driven wind characterized by a positive gradient near the surface and a negative gradient above. They also reproduced the laboratory experiment of Harris (1966). Their solution was confined to the WBL and to obtain those results they had to decrease the wave growth coefficient to five times compared to theoretical predictions.

Sullivan et al. (2008) took a different approach based on large-eddy simulation (LES) of the ABL. In the case of a following-swell they were able to reproduce a wind maximum at low levels above the surface and a small positive momentum flux up to the top of the boundary layer.

In the present study, the (possible) impact of a following-swell on the structure of the ABL at low wind speeds over the open ocean is investigated. To that end the model by Kudryavtsev and Makin (2004) is extended to the ABL by including the Coriolis force in the momentum conservation equation and an appropriate mixing length. As the present study is not aimed at a detailed description of the WBL, it is parameterized here in a simpler way than in Kudryavtsev and Makin (2004).

2 Generalized Ekman's Equations

Let us consider the atmospheric boundary layer above the ocean. Keeping in mind to explicitly account for the impact of waves on the structure of the ABL the generalized Ekman's equations are written in the form

$$\frac{\partial \boldsymbol{\tau}}{\partial z} - if(\boldsymbol{U} - \boldsymbol{G}) = 0 \tag{2}$$

with

$$\boldsymbol{\tau} = \boldsymbol{\tau}^t + \boldsymbol{\tau}^w, \tag{3}$$

where $\boldsymbol{U} = u + iv$ is the complex horizontal wind velocity, $\boldsymbol{\tau}^t = k\partial \boldsymbol{U}/\partial z$ is the turbulent stress, $\boldsymbol{\tau}^w$ is the wave-induced stress (stresses are normalized on the air density ρ_a), $\boldsymbol{G}$ is the geostrophic wind velocity with the magnitude $G = |\boldsymbol{G}|$, and f is the Coriolis parameter. The eddy viscosity k is traditionally expressed in the form

$$k = l\sqrt{\tau^t}, \tag{4}$$

where $\tau^t = |\boldsymbol{\tau}^t|$, l is the generalized mixing length, which for a neutrally stratified ABL can be written (e.g., Zilitinkevich and Esau 2005)

$$l^{-1} = (\kappa z)^{-1} + C_u \delta_E^{-1}. \tag{5}$$

In (5) κ is the von Karman constant, and

$$\delta_E = \frac{\kappa u_{*s}}{f} \tag{6}$$

is the scale of the Ekman layer, u_{*s} is the surface friction velocity, and C_u is a constant close to 2. The upper boundary condition is specified at the top of the ABL, $H = 2\delta_E$, and the direction of the geostrophic wind coincides with the x-axis, so that

$$z = H : u = G, \quad v = 0. \tag{7}$$

The lower boundary condition is specified at the height of the roughness length

$$z = z_0 : u = v = 0, \tag{8}$$

and at low wind speeds considered in this study the viscous roughness length is

$$z_0 = 0.1\frac{\nu}{u_{*s}}, \tag{9}$$

where ν is the molecular viscosity of the air.

3 Wave-Induced Stress

Equations (2)–(9) with $\boldsymbol{\tau}^w = 0$ describe the structure of the ABL above the ocean, where the impact of wind waves on the atmosphere is parameterized via the roughness length. The impact of swell is explicitly included via the wave-induced stress $\boldsymbol{\tau}^w$. In the wave boundary layer, a thin layer (compared to H) adjacent to the sea surface, the total stress can be split into turbulent and wave-induced parts according to (3) (Makin et al. 1995). The height of the WBL δ_W is defined as the height where the wave-induced stress becomes negligible compared to the turbulent stress. Following Makin and Kudryavtsev (1999) the wave-induced stress can be written as

$$\boldsymbol{\tau}^w = \boldsymbol{\tau}_s^w f(z), \tag{10}$$

where $\boldsymbol{\tau}_s^w$ is the wave-induced stress at the sea surface, and $f(z)$ is a decay function that equals 1 at the surface and $f(z) \to 0$ at $z \to \delta_W$. Swell could be well approximated by a monochromatic wave (e.g., Grachev and Fairall 2001) with the steepness AK (A is the amplitude, $K = g/C^2$ is the wavenumber, g is the acceleration due to gravity, and C is the phase speed). For a monochromatic wave propagating along the wind the wave-induced stress at the surface takes the form (Kudryavtsev and Makin 2004; Makin et al. 2007)

$$\tau_s^w = |\boldsymbol{\tau}_s^w| = \frac{1}{2}(AK)^2 C_\beta u_{*s}^2, \tag{11}$$

where C_β is the growth rate coefficient (not to be confused with the growth rate parameter $\beta = \rho_a \rho_w^{-1} C_\beta u_{*s}^2 C^{-2}$) defined as in Kudryavtsev and Makin (2004). Here, it is assumed that swell is aligned with the surface wind direction, a situation typical for swell regimes in the open ocean (Grachev and Fairall 2001). Let us rewrite Eq. 11 in the form

$$\tau_s^w = \alpha_c u_{*s}^2, \tag{12}$$

where

$$\alpha_c = \frac{1}{2}(AK)^2 C_\beta \tag{13}$$

can be recognized as the coupling parameter built on the surface friction velocity $u_{*s}^2 = \tau_s^t = |\boldsymbol{\tau}_s^t|$ so that

$$\frac{\tau_s}{u_{*s}^2} = 1 + \alpha_c. \tag{14}$$

The amplitude A is defined here as $A^2/2 = \overline{\eta^2}$, where $\overline{\eta^2}$ is the mean squared elevation of swell, and the significant swell height is defined as $H_s = 4(\overline{\eta^2})^{1/2}$ so that the significant height steepness $H_s K/2 = \sqrt{2}AK$. For a monochromatic wave the decay function scales with the height of the inner region δ_{IR}, and as shown by Makin and Kudryavtsev (1999) it can be written as

$$f(z) = \exp^{-z/\delta_{IR}} \cos\left(\frac{\pi}{2}\frac{z}{\delta_{IR}}\right), \tag{15}$$

where according to Cohen and Belcher (1999)

$$\delta_{IR} = \frac{c_{ir}}{K}, \tag{16}$$

which follows from rapid distortion theory above waves, and c_{ir} is a constant lying between 0.01 and 0.1. Here, the upper limit 0.1 is taken. Notice, that the decay function in the form (15) produces a pronounced minimum just above the inner-layer height δ_{IR}. The vertical oscillatory decay behaviour of the wave-induced flux reflects the nature of any oscillatory flow, in particular caused by the orbital velocities in the viscous fluid. Such behaviour is confirmed by numerical simulations (Makin and Kudryavtsev 1999). The height of the WBL δ_W as defined here would then be at the height where this minimum goes to zero. By specifying the swell parameters AK, C_β and K Eqs. (2)–(9) can be solved to obtain $\boldsymbol{U}(z)$ and $\boldsymbol{\tau}^t(z)$.

4 Results

Let us rewrite the Ekman's equations in the dimensionless form, choosing for scales G and g. It is easy to show that the solution of the problem will depend on one inner parameter $p_f = fG/g$, one parameter resulting from the definition of the roughness length $p_\nu = \nu g/G^3$, and two parameters that characterize the impact of swell: the coupling parameter α_c and the wave-age parameter $\Omega = (C/G)$ resulting from the definition of the inner region (IR) height δ_{IR}, Eq. 16. Notice that the dimensionless $\delta_{IR} = c_{ir}\Omega^2$. It is obvious that the coupling parameter defines the strength of the impact.

Fixing parameter p_f at the value corresponding to the geostrophic wind speed $G = 3\,\mathrm{m\,s^{-1}}$ the parameter p_ν is defined as well. The solution is searched for the main parameter α_c, with the fixed inverse wave-age parameter $\Omega^{-1} = 0.2$, a value that is typical of swell in the open ocean (Grachev and Fairall 2001). For $G = 3\,\mathrm{m\,s^{-1}}$ this gives swell propagating with the phase velocity equal to $15\,\mathrm{m\,s^{-1}}$ and with wavelength of 144 m. The direction of the swell propagation coincides with the surface wind.

The height of the atmospheric surface layer (ASL) is $h \sim 0.1H$, and normally $h > \delta_W$. In the ASL the total stress $\boldsymbol{\tau}$ is constant with height (within 20%). Four scenarios are possible.

(1) No-swell case. The wind profile is logarithmic and the turbulent stress is constant within the ASL. Above the ASL the wind speed monotonically increases to match the geostrophic

wind speed, and the turbulent stress goes to almost zero. In the Northern Hemisphere the surface wind turns to the left from the geostrophic wind at an angle 8° (Fig. 1, dashed lines).

(2) Swell exists, and the coupling parameter $\alpha_c > -1$ so that the total stress is positive; here $\alpha_c = -0.62$. The reduction in the total stress near the surface due to the negative wave-induced flux is partly compensated by the increase of the turbulent stress as compared to the no-swell case below the height of the IR. Above the IR the wave-induced stress is almost zero (apart from a small maximum) and the turbulent stress (still within the ASL) should decrease to the value of the total stress. As $\boldsymbol{\tau}^t \sim \partial \boldsymbol{U}/\partial z$ the u-component of the wind speed increases below δ_{IR} and decreases above forming a characteristic wind profile with a bump at the height of the IR, Fig. 1. Above the ASL the wind speed monotonically increases to match the geostrophic wind speed and the turbulent stress goes to almost zero. The angle between the surface and geostrophic wind reduces to 5°.

(3) Swell exists but the coupling parameter $\alpha_c < -1$ so that the total stress is negative. The example shown in Fig. 2 is for $\alpha_c = -1.25$. In this case the reduction in the total stress near the surface due to the negative wave-induced flux is again compensated by the increase of the turbulent stress as compared to the no-swell case below the height of the IR. At the height of the IR the turbulent stress has to go through zero to match the total stress, which is negative, and remains negative in the ASL. Above the ASL it monotonically varies from a negative value to zero. This implies that below the IR the gradient of the u-component of the wind speed should be positive and above the IR it is negative, as the wind matches the geostrophic wind at the upper boundary. The wind profile satisfying these conditions is shown in Fig. 2 with a pronounced bump ($\partial u/\partial z = 0$), $\max(u/G) = 1.25$ at the height of the IR $\delta_{IR} \approx 2$ m. This corresponds to Smedman et al. (1999) and Grachev and Fairall (2001), who found that the wind profile should have a maximum at a height below 10 m with a negative gradient above. The surface wind turns to the right from the geostrophic wind at an angle −7°. In this case swell considerably changes the structure of the ABL leading to an increased transport of momentum in the ASL. The negative wind gradient can be traced

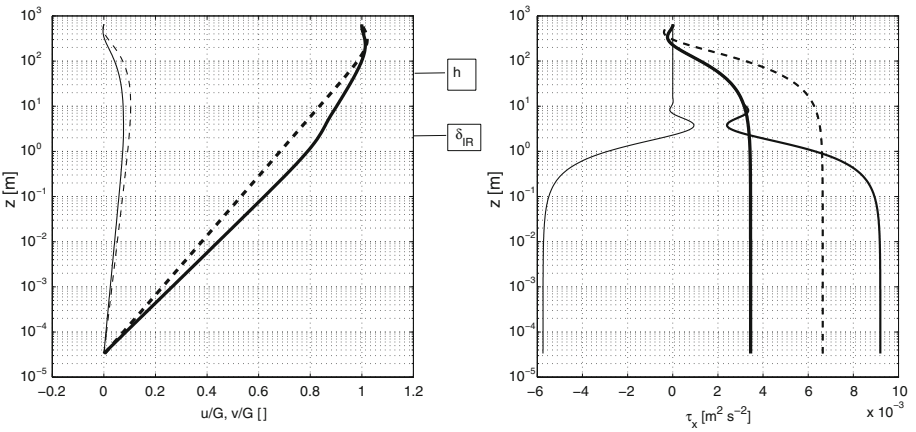

Fig. 1 *Left*. Wind-speed components. *Thick solid line*—u-component; *thin solid line*—v-component; swell is present, $\alpha_c = -0.62$ ($C_\beta = -500$, $AK = 0.05$). *Thick dashed line*—u-component; *thin dashed line*—v-component, no swell. *Right*. Stress components (only x-axis components are shown). *Thick solid line*—total stress; *medium solid*—turbulent stress; *thin solid*—wave-induced stress, swell is present. *Dashed line*—turbulent stress, no swell. The heights of the inner region δ_{IR} and the atmospheric surface layer h are shown by horizontal lines crossing the vertical axis

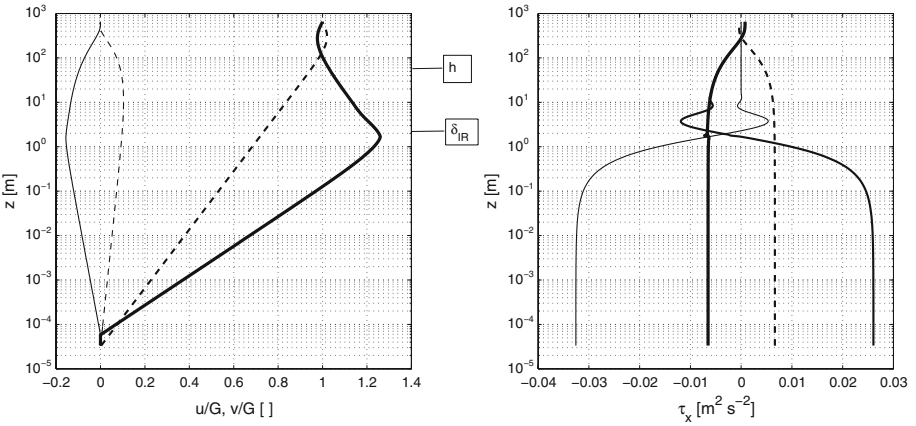

Fig. 2 The same as in Fig. 1, but for $\alpha_c = -1.25$ ($C_\beta = -1{,}000$, $AK = 0.05$)

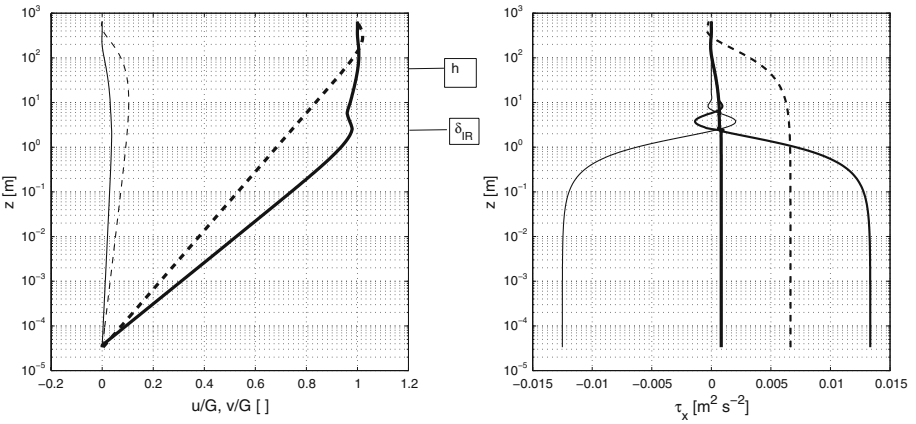

Fig. 3 The same as in Fig. 1, but for $\alpha_c = -0.94$ ($C_\beta = -750$, $AK = 0.05$)

to a height of about 200 m, corresponding to observations of Smedman et al. (1994). The geostrophic drag coefficient $CD_g = (u_{*s}/G)^2$ is considerably increased as compared to the no-swell case, from a value of 7.5×10^{-4} to about 3×10^{-3}. Notice that the drag coefficient estimated traditionally at 10-m height decreases and even becomes negative with a decrease in the swell coupling parameter, a feature observed by Guo-Larsen et al. (2003) and Sullivan et al. (2008).

With further decrease of the coupling parameter the ratio $\max(u/G)$ increases and the drag coefficient increases too. For $\alpha_c = -1.6$, $\max(u/G) = 1.7$ and $CD_g = 7 \times 10^{-3}$. Increasing the wind speed (for example, to $G = 5\,\mathrm{m\,s^{-1}}$) and keeping other parameters unchanged leads to an increase of the IR height ($\delta_{IR} \approx 6\,\mathrm{m}$) and a small decrease in $\max(u/G) = 1.2$ and $CD_g = 2.5 \times 10^{-3}$.

(4) Swell exists, the coupling parameter is close to -1, $\alpha_c \gtrsim -1$, so that the total stress is close to zero but slightly positive. The example shown in Fig. 3 is for $\alpha_c = -0.94$. Below the height of the IR the turbulent stress is positive matching the total stress at the height of the IR. Due to the fact that the wave-induced stress has an elevated positive maximum just

above the IR, and to keep the total stress constant, the turbulent stress goes through zero and becomes negative. At the height where the wave-induced stress turns to zero the turbulent stress matching the positive total stress again goes through zero from a negative to a positive value. This results in the wind profile shown in Fig. 3. The gradient of the u-component of the wind speed is positive below the IR, then it goes through zero to negative and becomes positive again, as the wind matches the geostrophic wind. The wind velocity profile is characterized by two bumps: one maximum at the height of the IR, and one minimum above the IR, which results from the elevated maximum in the wave-induced stress profile. The wind profile with such a shape was observed by A.S. Smedman (personal communication 2007) in the Baltic Sea with the exception that the maximum was located at about 10-m height. The observed peculiarities of the wind profile suggest that the elevated maximum in the wave-induced flux exists.

5 Discussion and Conclusions

This study shows that under certain conditions regulated by the swell parameters the impact of swell can be significant, changing the structure of the entire atmospheric boundary layer (ABL) and being especially pronounced in the surface layer.

The parameter that defines the strength of the impact is the coupling parameter α_c as defined by Eq. 13, and the most interesting case is when $\alpha_c < -1$. The total surface flux is then negative and the wind profile is characterized by a positive gradient inside the inner region (IR) and a negative gradient above the IR. This results in the pronounced bump at the height of the IR. The model results correspond at least qualitatively to measurements by Smedman et al. (1994, 1999) and Grachev and Fairall (2001). The question arises however – is this parameter realistic? The coupling parameter is a product of the swell steepness AK and the growth rate coefficient C_β. From data listed in Donelan et al. (1997) it is possible to conclude that the swell steepness $AK = 0.05 \div 0.1$ is realistic for the open ocean, so taking $AK = 0.05$ and $\alpha_c = -1.25$ results in $C_\beta = -1000$, while taking $AK = 0.1$ and $\alpha_c = -1.25$ results in $C_\beta = -250$. Theoretical values of C_β for a range of inverse wave-age parameter $0.1 \div 0.2$ are from -250 to -100 as calculated by the same wave boundary-layer model used by Kudryavtsev and Makin (2004). The problem is, however: can we apply results obtained by the wave-boundary layer model, which assumes the logarithmic wind profile within the constant-flux layer and which extends to the height corresponding to the wavelength, to the present situation where the wind profile is characterized by a bump rather close to the surface? That is not clear. If it is legitimate the theoretical values of C_β should be decreased by a factor of about 5 to obtain the correct values of α_c as already found by Kudryavtsev and Makin (2004).

On the other hand direct measurements of the total flux $\tau\rho_a$ by Grachev and Fairall (2001) give values of about $-0.002 \div -0.007\,\mathrm{N\,m^{-2}}$, which does not contradict the present study. Drennan et al. (1999a, b) report even higher values of the magnitude of the upward flux ($0.006 \div 0.03\,\mathrm{m^2\,s^{-2}}$) measured at height 12 m for a short swell of 60 m in length.

The form of the measured wind profile (Smedman et al. 1994) in the ASL and the existence of the negative wind gradient above 10 m (Smedman et al. 1999; Grachev and Fairall 2001) are in agreement with the model results, which also suggests that in nature the values of the coupling parameter are less than -1. Of course, there is also the possibility that mechanisms other than swell are responsible for the observed features of the wind profile. For example, according to Smedman et al. (1999), this peculiarity is caused by inactive turbulence, which is imported by pressure transport from layers in the upper parts of the ABL.

The characteristic spatial length of swell attenuation due to interaction with the wind is $L = -(\beta\omega)^{-1}C_g$, where $\omega = CK$ is the swell frequency and $C_g = C/2$ is the group velocity. For $\alpha_c = -1.25$ and parameters of swell taken in this study, L results in 100 km for $AK = 0.05$ and 400 km for $AK = 0.1$. The attenuation seems to be too large. On the other hand swell observed in studies (Munk et al. 1963; Snodgrass et al. 1966) had much lower frequency, up to 0.2 rad s^{-1} propagating at the phase speed of 50 m s^{-1}. Such swell will attenuate on scales of few thousand km.

In the definition of the height of the inner region δ_{IR}, Eq. 16, a constant c_{ir} regulates the vertical height of the IR and thus the occurrence of the bump ($\max(u)$) in the wind profile. The value 0.1 chosen here is the upper limit resulting from the rapid distortion theory (Cohen and Belcher 1999). Decreasing this value results in a decrease in the height of the bump in the wind profile. However, this does not change the conclusions of the present study. Increasing the constant increases δ_{IR} and the height of $\max(u)$, and with a value of 0.4, increases δ_{IR} to about 10 m, corresponding to the height of the maximum in the wind profile reported by A.S. Smedman (personal communication 2007). However, such a value of the constant then contradicts the results of the rapid distortion theory.

Summarizing: if the coupling parameter took on a value of -1 swell would have a significant impact on the entire atmospheric boundary layer. Indirect evidence points to the possibility of such a strong impact. However, no direct measurements of the growth rate parameter exist for fast swell, and the choice of the growth rate coefficient that leads to the values of the coupling parameter lower than -1 remains speculation. Measurements of Grachev and Fairall (2001) and Smedman et al. (1999) revealed a negative gradient of the wind speed above 10-m height, which points to the existence of the bump in the wind profile below this height. However, the exact height of this bump and whether or not it is related to the height of the inner region of swell is not known. Documented simultaneous measurements of swell and atmosphere parameters are few or lacking for very low wind speeds and high values of the wave-age parameter. Further experimental and theoretical research is needed to resolve the issues. At present the results obtained in this note should be taken with caution. Low winds and the presence of swell are typical for the tropical ocean regions, where an understanding of swell impact on the exchange processes at the air-sea interface is a potentially important issue in climate research.

Acknowledgements The Collaborative Linkage Grant ESP.NR.NRCLG 982529 by Public Diplomacy Division, Collaborative Programmes Section, NATO, and ONR grant N00014-08-1-0609 (Pr.No.: 08PR06145-00) are gratefully acknowledged.

References

Cohen JE, Belcher SE (1999) Turbulent shear flow over fast-moving waves. J Fluid Mech 386:345–371

Donelan MA, Drennan WM, Katsaros KB (1997) The air-sea momentum flux in conditions of wind sea and swell. J Phys Oceanogr 27:2087–2099

Drennan WM, Graber HC, Donelan MA (1999) Evidence for the effects of swell and unsteady winds on marine wind stress. J Phys Oceanogr 29:1853–1864

Drennan WM, Kahma KK, Donelan MA (1999) On momentum flux and velocity spectra over waves. Boundary-Layer Meteorol 92:489–515

Gent PR, Taylor PA (1976) A numerical model of the air flow above water waves. J Fluid Mech 77:105–128

Grachev AA, Fairall CW (2001) Upward momentum transfer in the marine boundary layer. J Phys Ocean 31:1698–1711

Guo-Larsen X, Makin VK, Smedman AS (2003) Impact of waves on the sea drag: measurements in the Baltic Sea and a model interpretation. The Glob Atmos Oceanogr Syst 9:97–120

Harris DL (1966) The wind-driven wind. J Atmos Sci 23:688–693

Kudryavtsev VN, Makin VK (2004) Impact of swell on marine atmospheric boundary layer. J Phys Oceanogr 34:934–949
Makin VK (1980) On energy transfer to waves. Izv Atmos Oceanogr Phys 16:382–384
Makin VK, Kudryavtsev VN (1999) Coupled sea surface-atmosphere model 1. Wind over waves coupling. J Geophys Res 104:7613–7623
Makin VK, Mastenbroek C (1996) Fluxes of momentum and heat above waves. In: Donelan MA, Hui WH, Plant WJ (eds) The air-sea interface. The University of Toronto Press, Toronto, pp 475–480
Makin VK, Kudryavtsev VN, Mastenbroek C (1995) Drag of the sea surface. Boundary-Layer Meteorol 73:159–182
Makin VK, Branger H, Peirson WL, Giovanangeli JP (2007) Stress above wind-plus-paddle waves: modelling of a laboratory experiment. J Phys Oceanogr 37:2824–2837
Munk WH, Miller GR, Snodgrass FE, Barber NF (1963) Directional recording of swell from distant storms. Phil Trans Roy Lond A 255:505–584
Smedman A-S, Tjernström M, Högström U (1994) Near-neutral marine atmospheric boundary layer with no surface shearing stress: a case study. J Atmos Sci 51:3399–3411
Smedman A-S, Högström U, Bergström H, Rutgersson A, Kahma KK, Pettersson H (1999) A case study of air-sea interaction during swell conditions. J Geophys Res 104:25833–25851
Snodgrass FE, Groves GW, Hasselmann KF, Miller GR, Munk WH, Powers WH (1966) Propagation of ocean swell across the Pacific. Phil Trans Roy Lond A 259:431–497
Sullivan PP, Edson JB, Hristov T, McWilliams JC (2008) Large-eddy simulations and observations of atmospheric marine boundary layer above nonequilibrium surface waves. J Atmos Sci 65:1225–1245
Yelland MJ, Taylor PK (1996) Wind stress measurements from the open ocean. J Phys Oceanogr 26:541–558
Yelland MJ, Moat BI, Taylor PK, Pascal RW, Hutchings J, Cornell VC (1998) Wind stress measurements from the open ocean corrected for airflow distortion by the ship. J Phys Oceanogr 28:1511–1526
Zilitinkevich SS, Esau IN (2005) Resistance and heat-transfer laws for stable and neutral planetary boundary layers: Old theory advanced and re-evaluated. Quart J Roy Meteorol Soc 131:1863–1892